Probiotics and Antimicrobial Proteins
https://doi.org/10.1007/s12602-025-10568-5

RESEARCH

# Mechanistic Divergence and Differential Antibacterial Potency of the Proline-Rich Antimicrobial Peptide B7-005 Across ESKAPE + E Pathogens

**Adriana Di Stasi[1] · Sara Capolla[1] · Martino Morici[3] · Sara Bozzer[1] · Max Berger[3] · Sabrina Pacor[1] · Thuy Duong Pham[2] · Roberto Spurio[2] · Attilio Fabbretti[2] · Paolo Macor[1] · Daniel N. Wilson[3] · Marco Scocchi[1] · Mario Mardirossian[1]**

Accepted: 25 April 2025


## Abstract

The urgent need for new antimicrobials is driving the optimization of proline-rich antimicrobial peptides (PrAMPs) as a basis for novel antibiotics to combat multidrug-resistant pathogens. The PrAMP B7-005 has emerged from this process, displaying a broader spectrum of activity compared to similar native PrAMPs and reduced reliance on the bacterial transporter SbmA for its action. While the compatibility and interactions of B7-005 with various mammalian cell types have been investigated, most information on its molecular mechanism of antibacterial action has so far been limited to *Escherichia coli*. In this study, we investigated the antimicrobial potency and mechanisms of action of B7-005 across the full panel of ESKAPE pathogens, with *E. coli* included for comparison (ESKAPE + E). The potential of B7-005 to eradicate these pathogens was evaluated in both planktonic and biofilm forms, revealing distinct bactericidal and anti-biofilm effects across the ESKAPE + E pathogens. B7-005's mechanism of action also varied depending on the target microorganism, ranging from intracellular inhibition of protein synthesis without membrane damage to varying levels of membrane permeabilization. Notably, B7-005 consistently inhibited protein synthesis across all ESKAPE + E pathogens, suggesting a possible combination of lytic and non-lytic mechanisms. Furthermore, biochemical analysis of its inhibitory effect on protein synthesis demonstrated that, despite acquiring membrane-destabilizing properties, B7-005 still blocks ribosome progression into the elongation phase, consistent with Class I PrAMPs. B7-005 thus retains the essential characteristics of native PrAMPs while offering a broadened spectrum of activity, highlighting its potential as a lead compound in the development of new antibiotics.

**Keywords** Antimicrobial peptide · Proline-rich · ESKAPE · Mode of action

## Introduction

The persistent use of antibiotics has led to the emergence of multidrug-resistant and extensively drug-resistant bacteria that render even the most effective drugs ineffective. The acronym ESKAPE refers to six nosocomial pathogens that exhibit multidrug resistance, including *Enterococcus faecium*, *Staphylococcus aureus*, *Klebsiella pneumoniae*, *Acinetobacter baumannii*, *Pseudomonas aeruginosa*, and *Enterobacter* spp., that are considered among the most concerning emerging threats for human health [1–3].

There are a number of antimicrobial resistance mechanisms exploited by nosocomial ESKAPE pathogens, including enzymatic inactivation, modification of drug targets, alteration of cell permeability, or enhancement of efflux pump expression [3]. New therapeutics to treat drug-resistant infections, particularly those caused by ESKAPE pathogens, which must circumvent these resistance mechanisms, are urgently needed [2]. Alternative therapies such as the use of antibiotics in combination, or with adjuvants, bacteriophages, nanoparticles, photodynamic light therapy, and antimicrobial peptides (AMPs) have been widely reported [2].

✉ Marco Scocchi
mscocchi@units.it

✉ Mario Mardirossian
mmardirossian@units.it

[1] Department of Life Sciences, University of Trieste, 34127 Trieste, Italy

[2] School of Biosciences and Veterinary Medicine, University of Camerino, 62032 Camerino, Italy

[3] Institute for Biochemistry and Molecular Biology, University of Hamburg, 20146 Hamburg, Germany

Published online: 05 June 2025

The AMPs, also known as host defence peptides, have recently captured attention as innovative drug candidates for the treatment of infectious diseases and as novel immunomodulatory therapies [4, 5]. AMPs are small polypeptides with potent antibacterial, antiviral, and antifungal activity that are ubiquitous in multicellular eukaryotes. Most plant and animal species express dozens of different AMP genes in epithelial tissues and in response to infection [6].

It was originally thought that membrane targeting and subsequent permeabilization was the only mechanism of action [7], but there is increasing evidence now that AMPs have other modes of action [7–9]. Proline-rich AMPs (PrAMPs) belong to this second category, since they are generally capable to cross the bacterial membrane without damaging it and to subsequently inhibit protein synthesis as the main mechanism of action, leading to a bactericidal outcome [10, 11].

At relatively low active concentrations, PrAMPs are internalized in susceptible Gram-negative bacterial cells exploiting the membrane transporters SbmA [12] and/or Yjil/MdtM [13] and then interfere with the bacterial translational machinery [10, 11, 14–17]. This correlates with a narrower spectrum of activity for PrAMPs compared to membrane-directed AMPs, as they tend to target a narrower set of Gram-negative bacteria. This is most likely due to the requirement for the presence of the specific membrane transport systems reported above, as well as to their intracellular mode of action [10, 18].

In a previous study, we systematically modified Bac7(1–16), an active N-terminal fragment of the natural peptide Bac7 [19], to identify amino acid residues essential for ribosome binding and to design new derivatives with enhanced antimicrobial properties [20]. The introduction of arginine (Arg) and tryptophan (Trp) residues at specific positions promoted antimicrobial activity against a broader range of bacterial pathogens than Bac7(1–16). Among the new compounds, B7-005 became independent of the SbmA transporter, and acquired a weak membrane-perturbing activity, while maintaining the full ability to inhibit protein synthesis in *E. coli* [20]. At the same time, B7-005 exhibited enhanced antibacterial activity against several bacterial pathogens without toxic effects on several types of human cells, both of tumoral or non-tumoral origin (MEC-1, HaCaT, A549, HUVEC, MG-63) [20–22]. Moreover, this peptide was effective in vivo, rescuing zebrafish embryos from *Escherichia coli* bacteraemia [22]. B7-005 deserves now a more comprehensive investigation of its efficacy and mode of action on clinically relevant bacterial species, e.g., the ESKAPE pathogens, broadening the knowledge that until now was collected mainly on *E. coli*.

Here, we systematically investigated the antimicrobial potency and molecular mechanism of B7-005 against ESKAPE pathogens, adding to this panel for comparison also *E. coli* (ESKAPE + E). Antibacterial and anti-biofilm assays were performed to characterize the activity spectrum and killing ability of the peptide. Membrane permeabilization and intracellular localization assays allowed the mechanism of action of the peptide against ESKAPE + E bacteria to be understood. Finally, the molecular details of the inhibition of the protein synthesis exerted by B7-005 toward the ESKAPE + E protein synthesis were obtained, drawing a clearer picture of B7-005 in view of its future development as a safe and effective antibacterial drug.

## Materials and Methods

### Peptides

B7-005 (Table 1) was synthesised by the company NovoPro Bioscience (Shanghai, China) using solid-phase synthesis with F-moc chemistry. It was then purified by RP-HPLC to a purity of > 95%, and its identity was confirmed checking its molecular weight by mass spectrometry. Fluorescently labelled derivative of B7-005 (B7-005-BY) was purchased by the company JPT (Berlin, Germany), where B7-005 with an additional Cys residue at the C-terminus (B7-005 Cys) was synthesised and purified as reported above. To fluorescently label the peptide, the BODIPY-FL Maleimide (BY) was reacted in solution to B7-005 Cys with the free thiol of the Cys to get the B7-005-BY. The fluorescent peptide was therefore re-purified and checked as above. All the peptides, including those subsequently labelled with the BODIPY, were synthesised with free C-termini. All the peptides were shipped lyophilised. Upon arrival, the peptides were freeze-dried three times in 10 mM HCl to replace the TFA with chloride. Then, the peptides were resuspended in sterile milli-Q water and quantified by spectrophotometer (Ultraspec 2100 pro, Amersham Bioscience). The concentration of the peptides was calculated according to literature data [23] for the calculation of molar extinction coefficients of the peptides using an in-house program and by measuring their absorbance at 214 nm and 280 nm according to

**Table 1** Amino acid sequence of PrAMPs B7-005 and B7-005-BY

| Peptide | Sequence | MW* | Charge* |
|---|---|---|---|
| B7-005 | WRIRRRWPRLPRPRWR | 2343.8 | + 8 |
| B7-005-BY | WRIRRRWPRLPRPRWRC-BY | 2861.2 | + 8 |
| Bac7(1–16)[a] | RRIRPRPPRLPRPRPR | 2076.5 | + 8 |
| Bac7(1–16)-BY[a] | RRIRPRPPRLPRPRPRC-BY | 2593.9 | + 8 |

[a]For comparison purposes, the sequences of Bac7(1–16) and Bac7(1–16)-BY are also shown

*Molecular weight and charge were calculated by using ProtParam tool of Expasy (https://web.expasy.org/cgi-bin/protparam/protparam)

Lambert–Beer's law, as well as exploiting the molar extinction coefficient of the BODIPY-FL for the B7-005-BY. The peptides were then stored at − 20 °C.

### *Bacterial* Cultures

The reference bacterial strains, originally purchased from American Type Culture Collection (ATCC) (Manassas, Virginia, USA) and from the Leibniz institute DSMZ (Braunschweig, Germany), used in this work were *Escherichia coli* ATCC 25922, *Klebsiella pneumoniae* ATCC 700603, *Acinetobacter baumannii* ATCC 19606, *Enterobacter cloacae* ATCC 13047, *Pseudomonas aeruginosa* ATCC 27853, *Staphylococcus aureus* ATCC 25923, and *Enterococcus faecium* ATCC 19434. All the bacterial strains were maintained at − 80 °C as glycerol stocks for storage. All the bacterial cultures were grown for all the experiments in sterile Müller-Hinton broth (MHB) or on agarized Müller-Hinton medium (MHA) (Difco Inc). For each experiment, the bacterial cultures were grown overnight (o/n) in 3 mL of MHB at 37 °C while shaking (140 rpm). The day after, overnight cultures of each strain were diluted 1:30 in a final volume of 10 mL of new MHB and incubated at 37 °C with agitation (140 rpm) for 1.5–2.5 h (mid-log phase) until an optical density (OD) of about 0.3 at 600 nm was reached. Then, the bacteria were diluted in new MHB to the desired for subsequent use.

### Calculation of Minimum Inhibiting and Bactericidal Concentration (MIC and MBC)

The minimum inhibitory concentration (MIC) assays were performed according to the guidelines of CLSI (Clinical and Laboratory Standards Institute). Briefly, the peptide was diluted in MHB to 128 μM to the final volume of 100 μL and dispensed in the first wells of a round bottom 96-well microtiter plate (Sarstedt, Milan, Italy). The peptide solution was then serially diluted two-fold in MHB, pipetting 50 μL of peptide solution in 50 μL of medium. Then, a mid-log bacterial culture (see above) was diluted in MHB to a bacterial load of $5 \times 10^5$ CFU/mL, and 50 μL of such suspension was added to each well of the plate (except the MHB sterility control wells), halving that way the final concentration of bacteria and peptides. The plate then was incubated overnight (o/n, 18 h) at 37 °C. The MIC value was calculated as the lowest concentration of compound resulting in the complete inhibition of visible bacterial growth. The minimal bactericidal concentration (MBC) was evaluated plating on MHA (Difco Inc.) plates 25 μL from each clear well of the MIC assay and incubating then the plates o/n at 37 °C for subsequent colony count. The MBC value was taken as the lowest concentration of compound reducing the viability of the initial bacterial inoculum by ≥ 99.9%. Results of MIC and MBC experiments are the mode of at least three independent experiments ($n \geq 3$).

### Bacterial Killing Kinetic

The kinetic of the B7-005 bactericidal activity was determined exposing a mid-log phase culture of the bacterial species reported above (see bacterial cultures) diluted to $2.5 \times 10^5$ CFU/mL in fresh MHB to concentrations of B7-005 corresponding to their MIC or 4 × MIC values. Bacteria were then incubated with the peptide at 37 °C for 1 h, 2 h, and 4 h. After the incubation, samples were taken and diluted serially in new MHB, plated on MHA in duplicates, and incubated o/n for counting viable colonies. An untreated control of the bacterial suspension, receiving water instead of peptide, was also considered for each time-point and underwent the same procedure as the other samples. The bacterial suspension was plated also at time zero of the incubation, to verify the starting bacterial load. Data represent the average ± SD of at least three independent experiments ($n = 6$).

### Bacterial Biofilm Inhibition/Eradication Assay

The biofilm inhibition/eradication assays were performed against all the bacterial strains reported above using plates from the MBEC Assay® Kit (Innovotech, Canada), consisting of a plastic lid with 96 pegs and a corresponding 96-well base.

To test the inhibition of new-biofilm deposition, serial two-fold dilutions of B7-005 were prepared in a volume 75 μL of MH broth in the wells of the plate considering a peptide concentration that was the double of the desired final-one. Each well was subsequently inoculated with 75 μL of a mid-log bacterial culture diluted in MHB to the concentration of $5 \times 10^5$ CFU/mL, to reach a final volume of 150 μL in the wells and halving therefore the concentration of bacteria and compound. As positive control for bacterial growth, some wells received no peptides. After 18 h of incubation at 37 °C, the whole lid with the pegs was transferred to a 96-well round- bottom plate (Sarstedt) containing 175 μL of PBS for 10 s to wash the biofilm on the pegs. After washing, the lid was transferred to a flat-bottomed black 96-well plate containing 175 μL of resazurin (TOX-8 kit, Sigma) diluted 1:20 (v/v) in MHB. The plate was incubated in the dark at 37 °C for at least 4 h to allow resazurine reduction. The viability of the biofilm was determined hourly by measuring the fluorescence at FLUOstar Omega-BMG Labtech spectrofluorometer ($\lambda_{ex} = 544$ nm, $\lambda_{em} = 590$ nm). The time required for the biofilm to metabolise resazurin varied depending on the bacterial species. Therefore, the time when the untreated control reached its maximum fluorescence was chosen as the time point for measurements.

Biofilm eradication activity was performed by inoculating in the wells of a multiwell plate with peg-lid (see above) 125 µL of mid-log bacterial cultures diluted in MHB to the concentration of $10^6$ CFU/mL and incubating the plates at 37 °C for 24 h to allow biofilm settling on the pegs. The day after, the lid with the pegs was transferred to a 96-well round-bottom plate (Sarstedt) containing 150 µL of PBS for 10 s to wash the pegs. The lid was then transferred to a second 96-well round bottom plate in which two-fold dilutions of B7-005 were prepared in 150 µL of MHB. After incubation at 37 °C for 18 h, the pegs were transferred again to a 96-well round- bottom plate (Sarstedt) containing 150 µL of PBS for 10 s to wash the pegs. Finally, the lid was transferred to a flat-bottomed black 96-well plate in which 175 µL resazurin (TOX-8 kit, Sigma), diluted 1:20 in MHB, was prepared. From this point, the protocol was performed as described above for the quantification of new biofilm deposition.

## Confocal Microscopy

A mid-log phase culture of *E. coli* ATCC 25922 was diluted to the final concentration of $10^6$ CFU/mL. Then, 500 µL of the bacterial suspension were exposed to 0.25 µM of the fluorescent compounds B7-005-BY [22], Bac7(1–16)-BY [24], or polymixin B-BY [24] for 10 min at 37 °C with shaking. Control bacteria received water instead of antimicrobials. At the end of the incubation, bacteria were centrifuged (5 min, 6200 × g), the supernatant was disposed, and bacteria were washed in a high-salt solution (400 mM NaCl, 10 mM Na-P buffer, 10 mM MgCl, pH 7.2) to remove all the peptide not firmly interacting with the membranes; then, bacteria were centrifuged again (5 min, 6200 × g). Finally, bacteria were resuspended in PBS and 5 µL of this suspension were put on a microscopy glass slide, covered with a coverslip and analysed using a confocal microscope Nikon Eclipse C1 si system equipped with a Nikon DS-Qi2 camera. Images were analysed using the Image-J software.

## Flow Cytometric Analysis of Membrane Integrity and Peptide Internalization

The flow cytometric assays were performed with Attune NxT® (ThermoFisher). The integrity of the bacterial cell membrane was assessed by measuring the uptake of propidium iodide (PI), whereby membrane permeabilization was calculated as % PI-positive cells, and the extent of membrane damage was quantified by observing the mean fluorescence intensity (MFI) of PI calculated on the whole bacterial population. Briefly, bacterial cultures of the species considered in the study (see point 3.3 of Materials and Methods) were diluted to a final concentration of $2.5 \times 10^5$ CFU/mL in MHB previously filtered at 0.2 µm, then incubated at 37 °C for 1 h in the presence of B7-005 concentrations corresponding to ¼ MIC and MIC values for each bacterial species. PI, at a final concentration of 10 µg/mL, was added to all samples 5 min before measurements. At the end of the incubation, the bacterial cells were analysed by flow cytometry. As a negative control for bacterial membrane damage, water was added to the bacterial suspension instead of peptide. Data analysis was performed with the Attune NxT Software. Data are expressed as means ± SD of three independent experiments ($n \geq 3$).

The uptake of the B7-005 peptide in bacterial cells was assessed using the fluorescent B7-005-BY and a quencher (Trypan Blue, TB, Sigma-Aldrich) to exclude the fluorescent signal of all the compound that was not internalized in bacteria. Mid-log phase bacterial cultures were diluted in filtered MHB to a final concentration of $2.5 \times 10^5$ CFU/mL. Bacterial cultures were then incubated for 30 and 60 min at 37 °C in a thermostat water bath in the presence of B7-005-BY at its respective ¼ MIC and MIC according to each bacterial species. TB, at the final concentration of 1 mg/mL, was added to bacterial culture 10 min before the measurements and incubated at room temperature. At the end of the incubation, samples were analysed by flow cytometry, evaluating the % of BY-positive cells. The extent of B7-005-BY internalization was quantified by observing the mean fluorescence intensity (MFI) of the unquenched BY signal calculated on the whole bacterial population. As a control for bacterial fluorescence, water was added to the bacterial suspension instead of peptide. The analysis of all the flow-cytometry data was performed with the Attune NxT Software, and results are expressed as means ± SD of three independent experiments ($n \geq 3$).

## Structural Analysis and Simulation

Circular dichroism (CD) spectroscopy was performed as previously reported [25, 26] using a J-715 spectropolarimeter (Jasco) with quartz cells of 0.1–0.2 cm path length. Peptides were prepared at a final concentration of 20 µM in either 10 mM sodium-phosphate buffer (SPB, pH 7.2–7.3) or 10 mM sodium dodecyl sulphate (SDS) in 10 mM SPB. Spectra were recorded from 190 to 240 nm at a scanning speed of 50 nm/min, with a data pitch of 0.5 nm and a bandwidth of 1.0 nm. Each spectrum represents the average of three scans.

The secondary structure of B7-005 was simulated using AlphaFold 3 [27] using standard settings for monomeric peptides.

## ESKAPE Pathogen Ribosome Preparation

For 70S ribosome purification, each bacterial strain was grown at 37 °C in 2 L of LB medium until mid-log phase. Cells were harvested by centrifugation at 7000 rpm

(12,000 × g) for 15 min at 20 °C (rotor JLA 8.1000) and resuspended in 50 mL of physiological solution (0.9% w/v of NaCl). Cells were pelleted again by centrifugation at 15,000 rpm (27,000 × g) for 10 min at 20 °C (rotor JA 25.50) and resuspended in 10 mL of Niremberg Buffer (NB) (10 mM Tris-HCI pH7.7, 60 mM NH4 Cl, 10 mM Mg acetate). The resuspended cells were snap-frozen in liquid nitrogen and stored at −80 °C until further use. Cells were thawed on ice and then lysed using a sonicator (Misonix 3000). Dithiothreitol (DTT) was added to the suspension to a final concentration of 1 mM, and the cell extract was cleared by centrifugation at 15,000 rpm (18,000 × g) for 30 min at 4 °C. The supernatant was subjected to ultracentrifugation at 80,000 rpm (320,000 × g) for 2 h at 4 °C (rotor S80-AT3), and the ribosome pellet was resuspended in a minimal volume of NB buffer with 1 mM DTT. The solution was further cleared of possible impurities by a final centrifugation at 15,000 rpm (18,000 × g) for 15 min at 4 °C. The ribosomes were quantified by Nanodrop ($A_{260\,nm}$). All the buffers described were filtered (MWCO = 0.2 µm) before use.

### In Vitro Translation Assay

The in vitro translation assay was carried out similarly as described previously [28], using the *E. coli* PURExpress system Δ ribosome (New England Biolabs (NEB)). Briefly, 1 µL of ESKAPE ribosomes in NB buffer isolated as described before, corresponding to 8 pmol of 70S, was used instead of *E. coli* ribosomes from the kit in 5 µL of PURExpress reaction mix, to which 1 µL of antibiotic solution was added. Each reaction contained 16 ng/µL of mRNA encoding the firefly luciferase (Fluc), which was in vitro transcribed from a pIVEX-2.3MCS vector containing the Fluc gene using T7 polymerase (Thermo Fisher Scientific). The reaction mix without the mRNA was first pre-incubated for 2 min at 32 °C while shaking (600 rpm); then, subsequent to mRNA addition, the reaction mix is incubated for 30 min at 32 °C while shaking (600 rpm). Reactions were stopped with 5 µL of kanamycin (50 mg/mL) and transferred into a 96-well microplate (Greiner Lumitrac, non-binding, white, chimney). Next, 40 µL of luciferase assay substrate solution (Promega, E1501) was added, and luminescence was measured using a plate reader (Tecan Infinite 200 PRO). Nuclease-free water was added instead of antibiotic as control. Absolute luminescence values were normalized using reactions without antibiotic. All assays were done as triplicates with individually prepared reaction mix.

### Toeprinting

Toeprinting reactions were performed as described previously [29]. In brief, reactions were performed with 6 µL of PURExpress in vitro protein synthesis system (NEB). The reactions were carried out on the ErmBL-toeprint template (5′-TAATACGACTCACTATAGGGAGACTTAAGTATAAGGAGGAAAAAATATGTTGGTATTCCAAATGCGTAATGTAGATAAAACATCTACTATTTGAGTGATAGAATTCTATC*GTTAATAAGCAAAATTCATTATAACC*-3′, Shine-Dalgarno is underlined; ORF start and stop codons are in bold, primer annealing site is in italic.), containing T7 promoter, a ribosome binding site, and the NV1* primer binding site. The template was generated by polymerase chain reaction of two overlapping 77-nt- and 78-nt-long primers. The reactions were supplemented with Retapamulin, Erythromycin, Bac7(1–16), or B7-005 in different concentrations as specified. The translation reactions containing the PURExpress system, ErmBL mRNA, NV*1 primer, and the respective compound were incubated for 20 min at 37 °C. The reverse transcription on the ErmBL-toeprint template was carried out using AMV RT and primer NV*1-Alexa 647 (5′-GGTTATAATGAATTTTGCTTATTAAC-3′). The translation reactions were incubated with AMV RT for 20 min at 37 °C. mRNA degradation was carried out by the addition of 1 µL of 5 M NaOH. The reactions were neutralized with 0.7 µL of 25% HCl, and nucleotide removal was performed with the QIAquick Nucleotide Removal Kit (Qiagen). The samples were dried under vacuum for 2 h at 60 °C for subsequent gel electrophoresis. The 6% acrylamide gels were scanned on a Typhoon scanner (GE Healthcare).

### Statistical Analysis

Data from at least three independent experiments were used, which were internal triplicate experiments. Differences between groups were evaluated using the unpaired Student *t* test, or the ANOVA test using SigmaPlot (Systat Software Inc.). Values of $p < 0.05$ were considered statistically significant.

## Results

### Antimicrobial Activity of B7-005 Toward the ESKAPE + E

B7-005 was tested against a representative strain of each ESKAPE group and of *E. coli* as well (Table 2), since previous investigation did not cover the whole ESKAPE group [20]. The broadening of the panel to *E. cloacae* and *E. faecium* indicated that B7-005 was active against all the pathogens included in the ESKAPE group, with MICs ranging from 2 µM to 32 µM (Table 2). Furthermore, MBC test indicated that B7-005 had bactericidal activity against all species under the tested conditions, excepting *E. faecium* (MBC > 64 µM), where under the tested conditions, inhibition of growth was observed but no killing activity.

**Table 2** Antimicrobial activity of B7-005 against a panel of reference strains of ESKAPE + E bacterial pathogens

| Bacteria strain | | B7-005 | |
|---|---|---|---|
| | | MIC (μM) | MBC (μM) |
| *E. coli* | ATCC 25922 | 1 | 2 |
| *E. cloacae* | ATCC 13047 | 8 | 16 |
| *S. aureus* | ATCC 25923 | 16 | 32 |
| *K. pneumoniae* | ATCC 700603 | 2 | 4 |
| *A. baumannii* | ATCC 19606 | 4 | 4 |
| *P. aeruginosa* | ATCC 27853 | 16 | 16 |
| *E. faecium* | ATCC 19434 | 32 | > 64 |

Results are the mode of at least three independent experiments ($n = 3$). MIC and MBC were recorded after 18 h of incubation at 37 °C

## Bactericidal Kinetic of B7-005 Toward the ESKAPE + E

To explore the bactericidal effect of B7-005, time-killing kinetic assays were performed exposing each of the ESKAPE + E pathogens to peptide concentrations corresponding to the MIC and fourfold MIC. B7-005 killed all the microorganisms, although to different extents. The peptide exerted potent and rapid time- and concentration-dependent bactericidal effect toward *E. coli* cells, whose viability decreased, e.g., by 2 $\log_{10}$ at MIC and by 4 $\log_{10}$ at 4 × MIC after 2 h (Fig. 1A).

Similar results were obtained with all the ESKAPE strains (Fig. 1B–G). Killing by B7-005 was very rapid also in *A. baumannii* and *E. cloacae*, where the peptide produced at least a 3-$\log_{10}$ reduction in number of viable cells at fourfold MIC, although the required concentrations corresponding to MIC and 4 × MIC increased with respect to *E. coli*. Also, *S. aureus* and *P. aeruginosa* displayed a similar drop in viability.

The killing activity of the peptide against *K. pneumoniae* and *E. faecium* was less rapid. A tenfold reduction in *K. pneumoniae* viable cells was observed at 4 × MIC within 4 h of incubation with B7-005, although occurring at relatively low concentration (8 μM). *Enterococcus faecium*, on the other hand, was poorly sensitive to B7-005, since a viability decrease similar to that observed for *K. pneumoniae* occurred only using very high concentration of peptide (128 μM) (Fig. 1B–G). For this reason, *E. faecium* was abandoned for subsequent assays in the current study.

## Effect of B7-005 on ESKAP + E Biofilm

The susceptibility of pre-existing biofilms of ESKAP + E (ESKAPE without *E. faecium* but including *E. coli*) to B7-005 was tested, to evaluate the capability of the peptide to eradicate them (Fig. 2). Furthermore, we tested the effect of the peptide toward the deposition of new biofilm by ESKAP + E (Fig. 3). In both these assays, the viability of the biofilm was monitored measuring

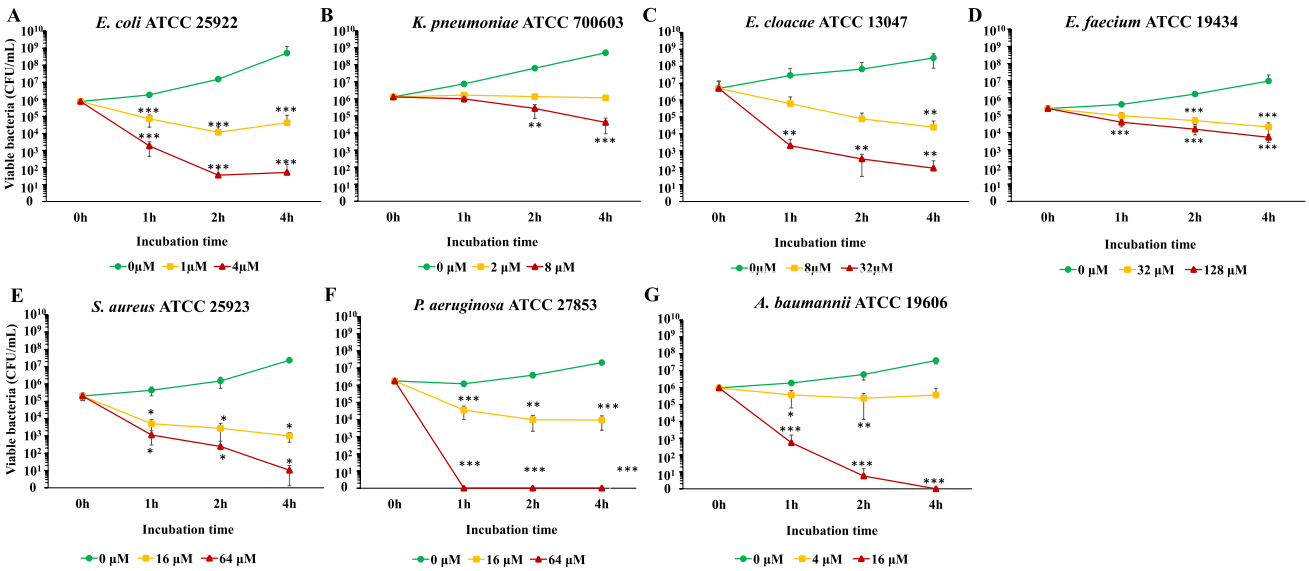


**Fig. 1** Time-killing kinetics of B7-005 against the ESKAPE + E bacteria. **A–G** Bacterial suspensions at mid-logarithmic phase diluted in MHB to a final concentration of 2.5 × $10^5$ CFU/mL were incubated at 37 °C in the presence of B7-005 at their respective MIC (yellow line) and 4 × MIC (red line), or in the absence of peptide (green line). Samples were then diluted in MHB, plated on MHA, and incubated overnight to allow the colony counts. Data are the average ± SD of at least three independent experiments in internal duplicate ($n = 6$). *$p <$ 0.05, **$p \leq 0.01$, and ***$p \leq 0.001$ versus the starting inoculum (test *t*-student)

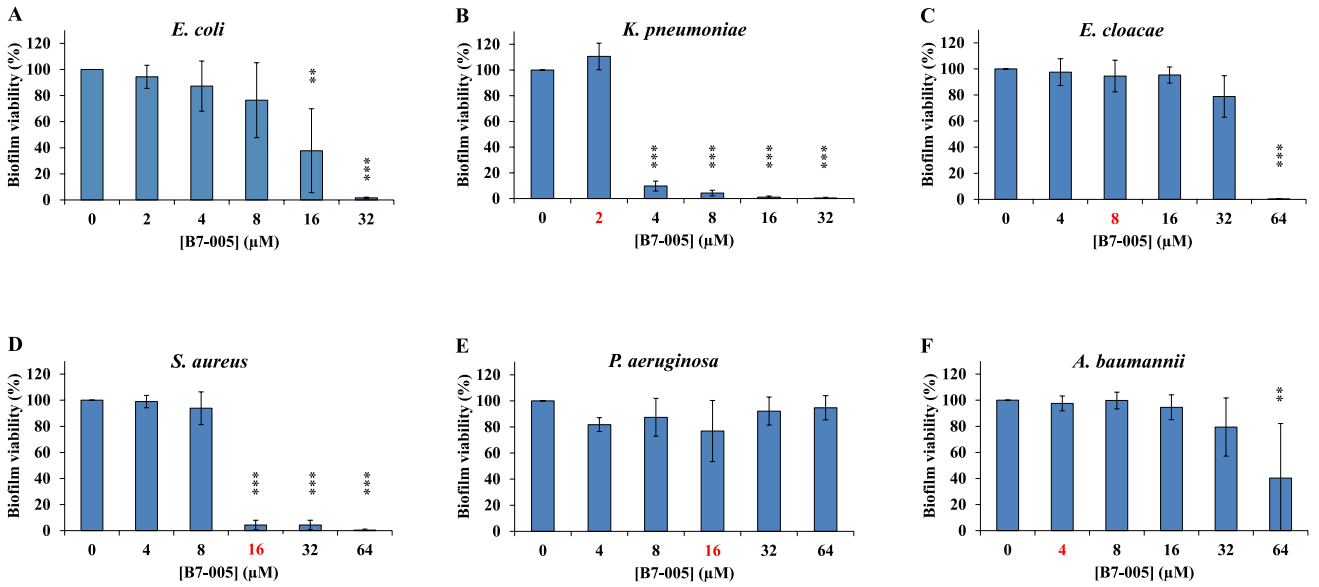


**Fig. 2** ESKAP + E biofilm eradication by B7-005. **A**–**F** The viability of the preformed biofilm was evaluated measuring fluorometrically the reduction of resazurin to resorufin after exposition to B7-005. Samples treated with water instead of B7-005 (indicated as 0 μM) were set as 100% of viability. The MIC of B7-005 for the different microorganisms is indicated in the graph as the red number except for *E. coli*, whose MIC value was 1 μM. Error bars are the standard deviations calculated on the average of at least three independent experiments performed as internal triplicates ($n \geq 9$). *$p < 0.05$, **$p \leq 0.01$, and ***$p \leq 0.001$ versus 0 μM (one-way ANOVA followed by Dunnett's multiple comparisons test)

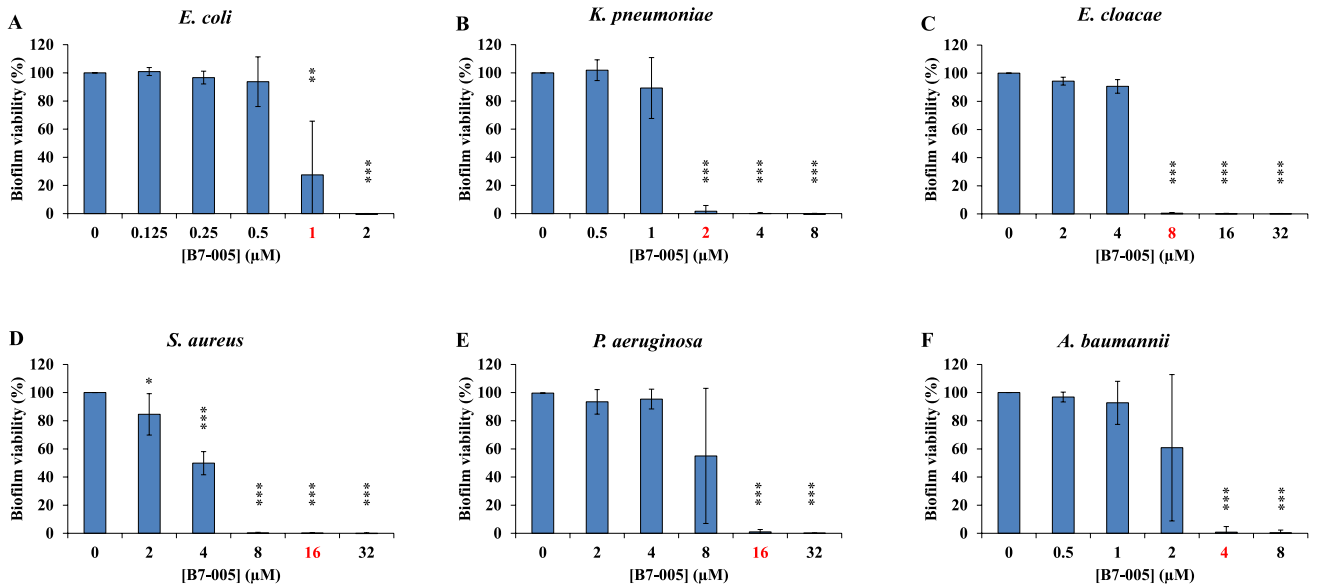


**Fig. 3** Inhibition of ESKAP + E biofilm deposition by B7-005. **A**–**F** The viability of the biofilm was evaluated measuring fluorometrically the reduction of resazurin to resorufin after exposition to B7-005. Samples treated with water instead of B7-005 (indicated as 0 μM) were set as 100% of viability. The MIC of B7-005 is indicated in the graph as the red number, this is not shown for *E. coli*, MIC = 1 μM. Error bars are the standard deviations calculated on the average of at least three independent experiments performed as internal triplicates ($n \geq 9$). *$p < 0.05$, **$p \leq 0.01$, and ***$p \leq 0.001$ versus 0 μM (one-way ANOVA followed by Dunnett's multiple comparisons test)

fluorometrically the reduction of resazurin to resorufin in the medium. B7-005 was administered toward each bacterial species with respect to its MIC, exploring two-fold multiples and sub-multiples of the inhibiting concentration, but not exceeding the concentration of 64 μM.

A minimum biofilm eradicating concentration (MBEC) of B7-005 was clearly identified for four bacterial species out of six. B7-005 had the highest effect toward *K. pneumoniae*, since a massive decrease of biofilm viability was observed already at 4 μM (2 × MIC) (Fig. 2B). The biofilm of *S. aureus* was also affected by B7-005 (Fig. 2D) since it was almost totally eradicated already at MIC (16 μM), even though the corresponding concentration *per se* was higher than for *K. pneumoniae* and *E. coli*. It is worth noting that although *E. coli* was the most sensitive pathogen to B7-005 in its planktonic form, once organized in a preformed biofilm, it was eradicated by the compound only at 32 μM (= 32 × MIC) (Fig. 2A). The biofilm of *E. cloacae* was eradicated at 64 μM. Although this represented a lower MIC-ratio compared to *E. coli* (8 × MIC), the MBEC for *E. cloacae* was among the highest observed (Fig. 2C). At last, the same concentration of B7-005 (64 μM) resulted only in a non-significant reduction in the viability of the *A. baumannii* biofilm (Fig. 2F), while it had no effect on the *P. aeruginosa* biofilm (Fig. 2E).

On the other hand, B7-005 affected the deposition of new bacterial biofilm in all ESKAPE, with little differences among the diverse species. The minimum biofilm inhibiting concentration (MBIC) of B7-005 was superimposable or very close to MIC of B7-005 toward each strain. There was negligible biofilm deposition by all bacterial species (Fig. 3B–F) in the presence of B7-005 at their respective MIC apart from *E. coli* (Fig. 3A), that needed 2 × MIC to experience the complete block of the biofilm deposition (Fig. 3A). On the other hand, the deposition of biofilm by *A. baumanni* was impaired already at MIC (= 4 μM). Finally, ¼ MIC was sufficient to B7-005 to reduce the biofilm deposition by *S. aureus*, that was then completely inhibited at ½ MIC (i.e., 4 μM and 8 μM, respectively) (Fig. 3D).

## B7-005 Enters the Cytosol of *E. coli*

Different to other Bac7 derivatives or homologues, there was no direct indication that B7-005 was internalized by bacteria. To address this point, *E. coli* ATCC 25922 cells were treated with a B7-005 derivative labelled with the fluorophore BODIPY-FL (B7-005-BY) and the localization of the peptide was evaluated by confocal microscopy on living bacteria. To have a comparison, fluorescent derivatives of the PrAMP Bac7(1–16) and of the antibiotic polymyxin B were used, as reference for an antimicrobial compound targeting cytosolic bacterial structures or acting on the microbial membranes, respectively (Fig. 4). Microscopic inspection of the mid cross-section of *E. coli* cells indicated that the fluorescent B7-005 was evenly distributed in the cytosol (Fig. 4A). B7-005 did not display the tropism for membrane displayed by polymyxin B (Fig. 4B), but, on the other hand, it stained *E. coli* dissimilarly than Bac7(1–16), which appeared entirely associated with cytosolic structures (Fig. 4C). Microscopy data are therefore in agreement with the hybrid mode of action previously suggested for B7-005, mainly relying on the targeting of protein synthesis upon internalization in the bacterial cytosol but also not-neglectable encompassing interactions with the bacterial membranes causing their destabilization and/or mild permeabilization [30].

## Mechanism of B7-005 on ESKAP + E Cells: Toward or Through the Bacterial Membrane?

To explain the differences in sensitivity to B7-005 among microorganisms (see Fig. 1), the antimicrobial mechanism exerted by B7-005 toward ESKAP + E was investigated by flow cytometry. The membrane integrity of bacteria exposed to B7-005 was evaluated measuring the uptake of propidium iodide (PI), a marker of compromised cell membranes. In

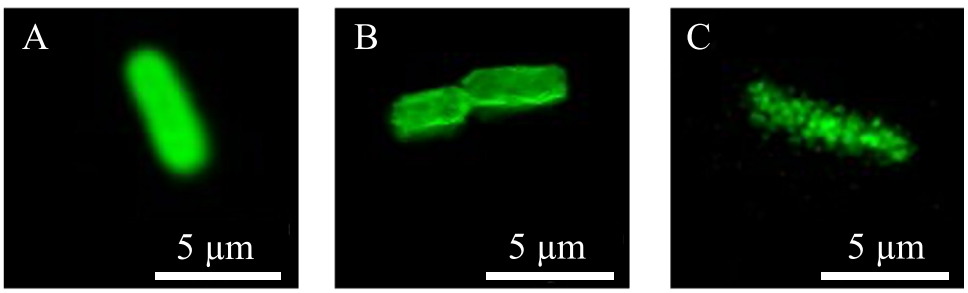


**Fig. 4** Confocal microscopy of *E. coli* cells. Bacteria were treated with fluorescent derivatives of **A** B7-005, **B** polymyxin B, and **C** Bac7(1–16). All the compounds were used at one-fourth of their respective MIC on *E. coli* ATCC 25922, i.e., 0.25 μM for both the compounds

parallel, the capability of B7-005 to enter the bacterial cell was also quantitatively evaluated using B7-005-BY, a fluorescent derivative of the peptide. All the bacterial species were treated with the peptide at concentrations corresponding to their relative ¼ MIC and MIC. To quantify not only the fraction of the cell population that became positive to the PI and B7-005-BY after treatment but also the extent of internalization of PI and B7-005-BY in the cell population, we measured the percentage of positivity to the fluorescent molecules as well as the mean fluorescence intensity (MFI) across the entire bacterial population.

B7-005 was not membrane-permeabilizing toward *E. coli* and *K. pneumoniae*, since less than 10% of their cellular population was positive to PI, even at MIC and after 2 h of exposure (Fig. 5A–B, upper panels). Moreover, under these conditions, the MFI of PI associated to bacteria was barely measurable or very low, respectively for *E. coli* and *K. pneumoniae*, suggesting that no damage occurred to the membrane (Fig. 5A–B, lower panels). On the other hand, after already 1 h of exposure to B7-005 at MIC, a high percentage of *E. cloacae*, *S. aureus*, *P. aeruginosa*, and *A. baumannii* populations was positive to PI (Fig. 5C–F, upper panels) suggesting that B7-005 destabilized the plasma membranes. The MFI of PI-treated cells however scarcely paralleled the number of PI-positive cells. Minimal fluorescence was in fact associated to *S. aureus* cells although ~80% of the population was PI-positive. This may indicate a scarce uptake of PI in the bacterial cells and suggesting therefore that the membrane was compromised but not dramatically damaged. On the other hand, the percentage of PI-positive cells in *E. cloacae*, *P. aeruginosa*, and *A. baumannii* was similar or lower compared to *S. aureus*, respectively, suggesting that a smaller portion of the bacterial population was affected by the membrane permeabilizing activity of B7-005. However, the MFI of PI-positive cells in *E. cloacae*, *P. aeruginosa*, and *A. baumannii* was considerably

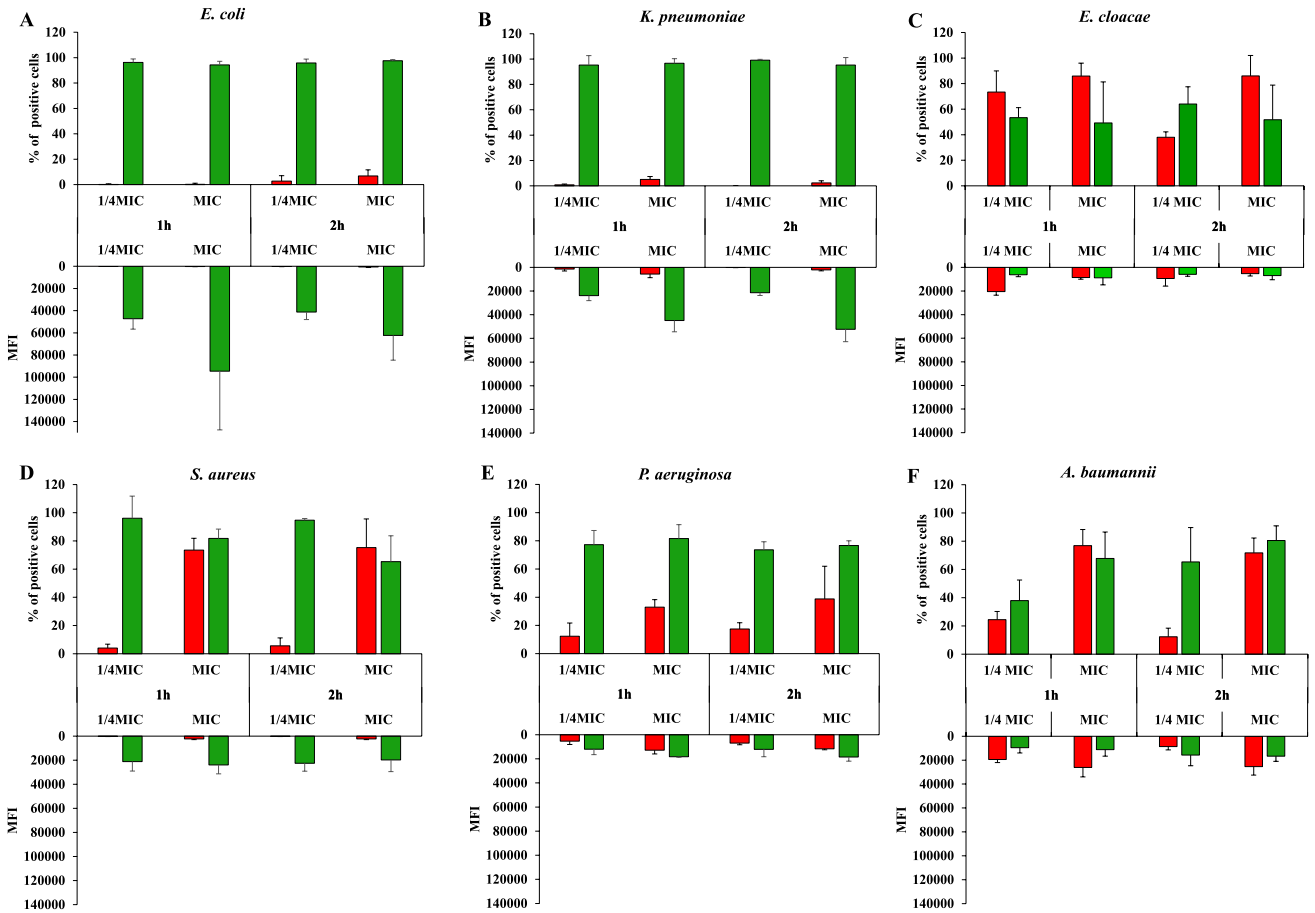


**Fig. 5** Membrane-damaging activity and uptake of B7-005 in *ESKAPE+E* evaluated by flow cytometry. Permeabilization of the bacterial membrane in the presence of B7-005 after 1 h or 2 h of exposition, assessed by uptake of propidium iodide (PI), (red bars). Internalization of B7-005, assessed using a fluorescent derivative and limiting the signal only to the intra-bacterial peptide (green bars). B7-005 was used, toward any bacterial specie, at its respective ¼× MIC and MIC. For both PI and fluorescent B7-005, the percentage of fluorescent bacterial cells (%, upper panels) and the mean fluorescence intensity (MFI, lower panels) over the population were measured. Error bars are the standard deviations calculated on the average of at least three independent experiments ($n \geq 3$)

higher than in *S. aureus*, suggesting a enhanced uptake of PI in these cells, that may reflect broader and more critical membrane damages (Fig. 5D–F, lower panels).

To determine whether B7-005 could enter bacterial ESKAP + E cells, the quencher trypan blue (TB) was used to quench extra-cellular fluorescence and to measure the signal of the intra-bacterial peptide only. Near 100% of the whole *E. coli* and *K. pneumoniae* populations became positive to B7-005-BY in the presence of TB, indicating efficient entering of the peptide at both inhibitory and sub-inhibitory concentrations (Fig. 5A–B, upper panels). *Escherichia coli* and *K. pneumoniae* also displayed a marked increase of MFI of B7-005-BY associated with bacterial cells suggesting an important uptake by *E. coli* and *K. pneumoniae*. On the other hand, the populations of all the other bacteria did not reach the same level of positivity to B7-005-BY and displayed lower MFI associated to bacteria. The peptide therefore was not internalized by the totality of the bacterial population, and if internalized, the amount of intra-bacterial peptide was lower than in *E. coli* and *K. pneumoniae*, suggesting less efficient internalization. However, it has to be considered that the proper evaluation of B7-005 uptake may be hampered if the bacterial membrane was damaged, allowing possible passive entering of peptide but also of the quencher.

In a bigger picture, these results indicate that B7-005 exerted a mainly non-lytic mode of action after internalization only toward *E. coli* and *K. pneumoniae*. On the other hand, the mechanism of B7-005 on *E. cloacae*, *S. aureus, P. aeruginosa*, and *A. baumannii* likely mainly relies on membrane permeabilization.

## B7-005 Does Not Adopt Canonical Secondary Structures

To investigate if the membranolytic mechanism displayed by B7-005 toward four microorganisms out of six may be related to its secondary structure, circular dichroism (CD) analyses were carried out to get conformational hints on this peptide. B7-005 was analysed in aqueous environment in the presence or in the absence of sodium dodecyl sulphate (SDS) micelles, to provide a first simple approximation of an anionic amphipathic environment such the bacterial membrane is (Figure S1A). The spectrum of B7-005 in buffer displayed characteristics of the polyproline II helix, like the overall shape, the minimum near 205 nm, and the maximum at 230 nm [31]. In partial agreement with CD, a structural simulation performed by AlphaFold 3 [27] excluded α-helix or β-sheet structures and predicted a horseshoe-like structure for B7-005, displaying three bends, in correspondence of each proline (Pro), and supporting the importance of prolines on the structure of this peptide. The SDS micelles then modified the conformation of B7-005, but we could not unambiguously assign the peptide to any of the canonical secondary structures. However, the clear modification of the CD spectrum of the B7-005 in the presence of detergent with respect to buffer alone, suggested that the peptide interacted with micelles.

## B7-005 Inhibits the Translation Activity of ESKAPE Ribosomes

B7-005 inhibits protein synthesis in *E. coli* lysates [30]. However, its capability to block the protein synthesis in other bacterial species was unknown. To investigate this point, in vitro protein synthesis was performed combining functional ribosomes of ESKAPE + E, extracted and purified from each of the pathogens, with the commercial purified translational machinery of *E. coli* depleted of the ribosomes (PURExpress, NEB), restoring therefore a complete functional translational machinery, analogous to that done previous for *Bacillus subtilis* ribosomes [32, 33]. In vitro protein synthesis was performed in the presence or in the absence of B7-005, evaluating its effect on the production of a luciferase as reporter. B7-005 impaired the production of luciferase in all the bacterial systems; however, differences in efficiency were observed among them (Fig. 6). Data on *E. coli* confirmed the potential of B7-005 as inhibitor of the protein synthesis and the peptide was similarly very effective also on *K. pneumoniae* ribosomes. Unexpectedly, the peptide performed efficiently also on *E. faecium* ribosomes, indicating that the low sensitivity of this bacterial specie to B7-005 cannot be attributed to differences in the ribosomes. *Acinetobacter baumanni* ribosomes were still very sensitive to B7-005, although the inhibition of protein synthesis was slightly less efficient than observed on *E. coli* and *K. pneumoniae*. Lastly, ribosomes of *S. aureus*, *E. cloacae*, and especially *P. aeruginosa* were inhibited by B7-005 with minor efficacy. It is worth noting that *E. coli* and *K. pneumoniae*, the only bacterial species affected by the peptide by a genuinely non-lytic mode of action (Fig. 5), were characterized also by a very strong inhibition of protein synthesis by B7-005.

## B7-005 Prevents *E. coli* Ribosomes from Entering the Elongation Phase

To investigate which step of protein synthesis was affected by B7-005, we performed a toe-printing analysis using *E. coli* ribosomes as a model. With this method, we monitored the position of bacterial ribosomes on a mRNA template in the presence of B7-005 as well as other molecules used as reference, i.e., another PrAMP and common antibiotics [16]. At a concentration of 5 μM, B7-005 stalled the ribosomes at the AUG codon, producing a band profile similar to that of

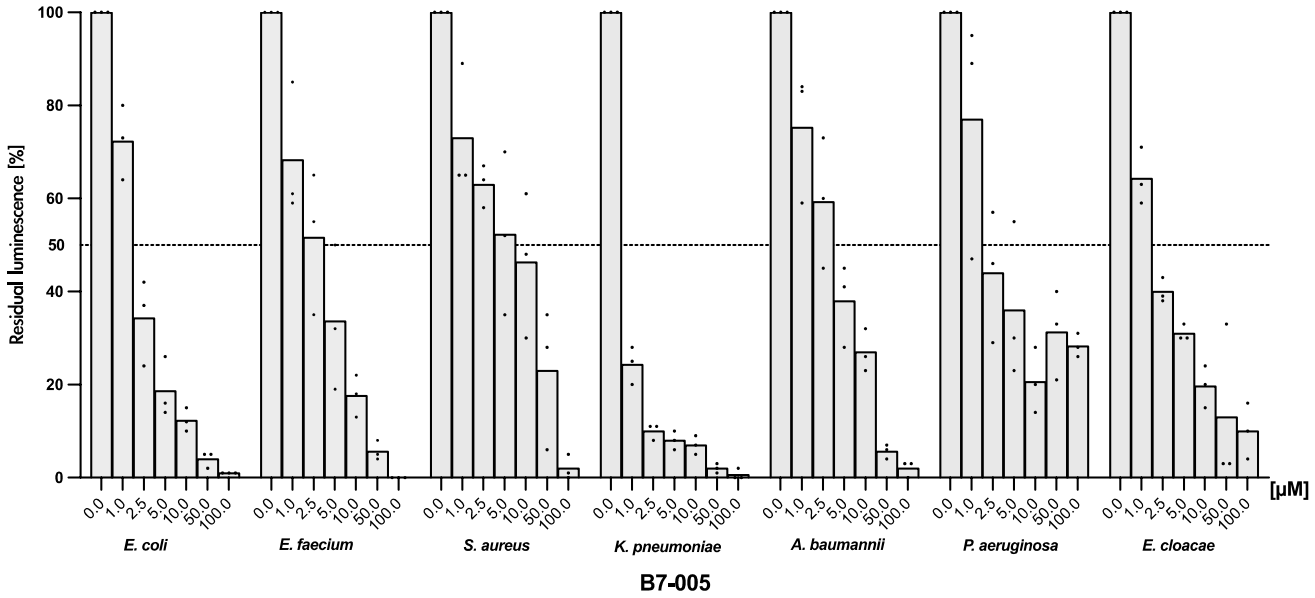


**Fig. 6** Inhibition by B7-005 of in vitro protein synthesis performed using *E. coli* and ESKAPE purified ribosomes to complement the ribosome-depleted transitional machinery of *E. coli*. Potency of inhibition was evaluated as a reduction in the luminescence signal from the FluC reporter luciferase (PURExpress, NEB). Controls receiving water instead of B7-005 were set as 100% of efficacy for each different system. Histograms represent the mean of independent triplicates ($n \geq 3$), whose single results are reported as black dots

the antibiotic retapamulin and of the PrAMP Bac7(1–16), both compounds preventing *E. coli* ribosomes from entering the elongation phase of translation [34, 35] (Fig. 7). The increase of B7-005 concentration from 5 to 50 μM revealed a switch in the mode of action of the peptide toward the ribosomes. In fact, in the presence of high amounts of peptide, the toeprint profile of B7-005 no longer indicated a prevalent inhibition of ribosomes by stalling them at the AUG codon. Instead, data suggested an impairment of the proper assembly of initiation complexes. This phenomenon was credible, as it had already been observed for other mammalian PrAMPs [35–37]. Overall B7-005, despite the insertion of tryptophan in its sequence and the subsequent modification of its chemico-physical properties, maintained the mechanism of ribosome inhibition typical of mammalian PrAMPs, i.e., inhibiting the elongation phase.

## Discussion

The ESKAPE + E pathogens represent a worrisome upcoming concern for global public health [1]. In this study, we tested the antimicrobial activity of B7-005, an artificial 16-amino-acid-long PrAMP, towards all of these pathogens, since previous investigation never used this whole panel of pathogens in parallel [30]. Our results showed that B7-005 exhibits inhibitory and bactericidal activity against a representative strain of each pathogen at low to mid micromolar concentrations, with the sole exception of *E. faecium*, which was poorly affected by the peptide. Moreover, we showed that B7-005 acts quickly, killing bacteria within a few hours of treatment.

The rapid bactericidal action is a highly desirable property for an antimicrobial, since small peptides like B7-005 typically have a rather short half-life in human serum due to fast renal clearance [38], as it has been already observed for some PrAMPs [38, 39]. On the other hand, the in vivo inactivation due to proteolytic cleavage, which often affects peptide drugs [38–40], is a minor concern for B7-005, since the peptide resisted the contact with human serum retaining most of its antimicrobial efficacy [22, 30].

Overall, B7-005 was active also against the sessile forms of some ESKAPE + E pathogens, displaying MBEC < 64 μM toward four bacterial species out seven, although a low MIC was not always predictive of a low MBEC. Unexpectedly, the biofilms of *E. coli* and *A. baumanni*, both very sensitive to B7-005 in planktonic form, were not easily eradicated. On the contrary, *S. aureus* biofilm was eradicated at MIC. This capability of B7-005 to affect contemporarily the motile and the sessile forms of *S. aureus* is a desirable feature for fighting this pathogen during an infection. However, the lowest MBEC was observed with *K. pneumoniae*, one of the bacteria with lowest MIC, whose biofilm was eradicated at low concentration. B7-005 therefore performed better toward *K. pneumoniae* biofilm than the related PrAMP Bac7(1–35), but also than the unrelated alpha-helical BMAP-27, displaying MBEC 8- and 16- fold higher than B7-005, respectively [41]. Given the clinical relevance of *K. pneumoniae* pathogenic

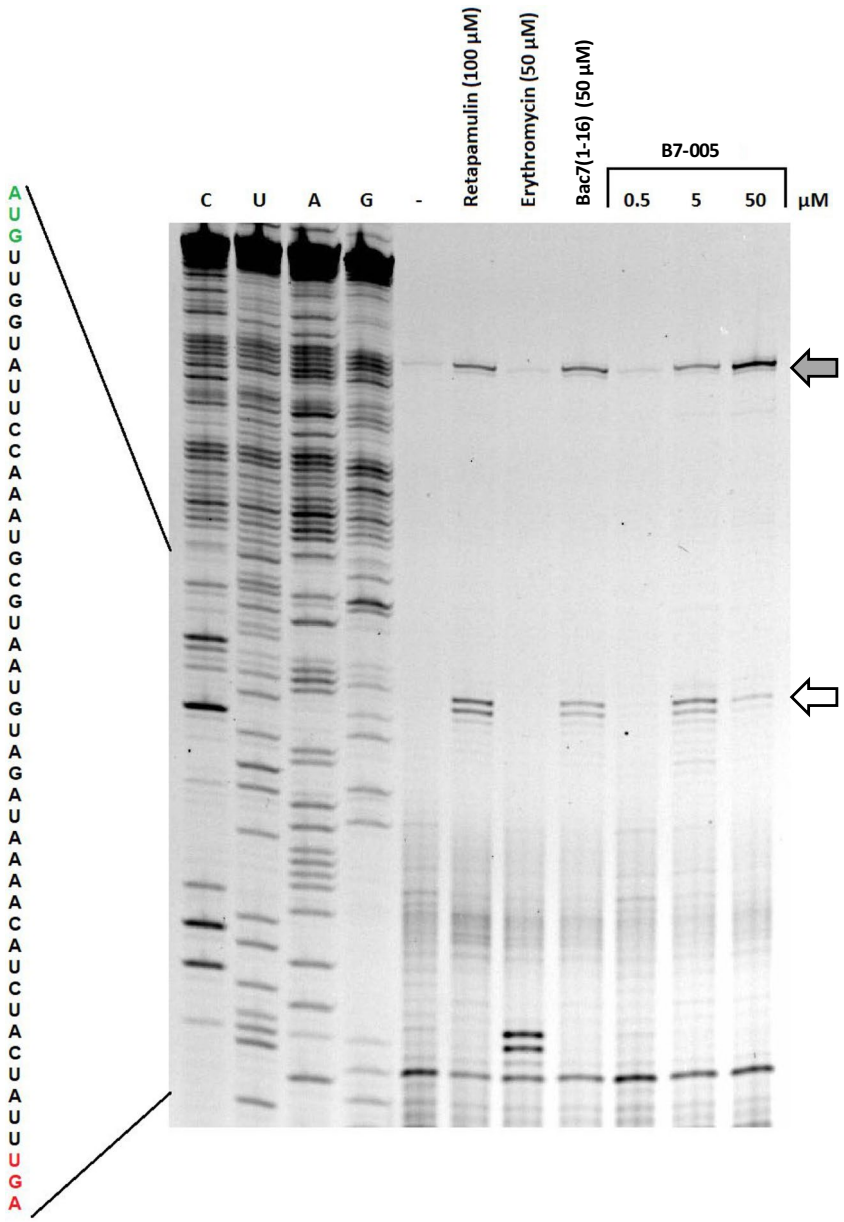


**Fig. 7** Block of in vitro protein synthesis by B7-005 monitored by toe-printing. Fluorescence visualization of a polyacrylamide gel of toe-printing reactions performed in the absence or presence of increasing concentrations of the peptide B7-005. Water, instead of antibiotics or peptide, was added to a reaction mixture as a control (lane -). Retapamulin and Bac7(1–16) were used for comparison as an antibiotic and a PrAMP, respectively, inhibiting the elongation and stalling ribosomes at the AUG site (white arrow). The position of the reverse transcription band corresponding to the full-length mRNA is indicated by the grey arrow. The lanes labelled C, U, A, and G show the DNA sequencing of the template

biofilms [42], B7-005 may represent a resource to fight this microorganism, although further studies will be needed to clarify the mechanism of this success. In fact, it is not clear which mechanism was exploited B7-005 to affect *K. pneumoniae* biofilm among the several ones known for AMPs [43] or even for PrAMPs, e.g., Bac7(1–35), that was proposed to interact with and collapse the polysaccharidic matrix of the *K. pneumoniae* biofilm leading to its disaggregation [44].

This work successfully investigated the mechanism by which B7-005 affects the planktonic target bacteria, an aspect previously only partially explored in *E. coli* [30] and completely unknown in the other ESKAPE pathogens. We tested membrane permeabilization, peptide penetration into the cytoplasm, and the in vitro capability of B7-005 to arrest protein synthesis. Overall, B7-005 shows relevant variation in its activity across different bacterial species, highlighting

a marked difference in the killing mechanisms toward *E. coli* and *K. pneumoniae* compared to the other bacteria.

Previously, we showed that B7-005 remained an effective inhibitor of the bacterial protein synthesis, but it also gained the tendency to interact with the bacterial membrane, moderately increasing its permeability at four to eight times the MIC [30]. The current work confirms this antimicrobial mechanism of B7-005 against *E. coli* and indicate that *K. pneumoniae*, another member of the *Enterobacteriaceae*, is affected similarly by the peptide. Both *E. coli* and *K. pneumoniae* internalized the peptide at MIC (1–2 μM) without membrane permeabilization, and their protein synthesis was effectively inhibited by B7-005 with comparable potential, as demonstrated by in vitro translation assay using purified ribosomes (Fig. 6). Moreover, confocal microscopy confirmed that B7-005 enters the cytosol of *E. coli* (Fig. 4), consistently with the behaviour of closely related mammalian PrAMPs, such as Bac7(1–35) [12], its shorter fragments [24], and Tur1 A [36]. However, unlike these other PrAMPs, a significant amount of B7-005 persistently remained on the bacterial envelope (Fig. 4) confirming that this peptide has higher affinity for the bacterial membrane compared to the native compound Bac7(1–16) [30]. The presence of three Trp residues in the sequence of B7-005, unlike in other PrAMPs, explains its higher membrane affinity and may account for its increased tropism for bacterial membranes, particularly relevant toward some bacterial species. Analysis of circular dichroism supported the interaction of B7-005 with the biological membranes although it did not allow for a complete clarification of its secondary structure (Figure S1A). The CD spectrum of the peptide in phosphate buffer resembled that of a type II polyproline helix [31], although the number of Pro in B7-005 sequence is limited to three residues out of 16. However, the charged side-chains of the 8 Arg may interact with the aqueous environment, stabilizing the polyproline helix even in spite of a moderate number of Pro in the sequence. Also, the preponderance of bulky residues in the sequence (8 Arg and 3 Trp) may impair, by steric hindrance, other structures which are usually promoted by prolines, like β-turns. Simulation with AlphaFold predicted a bent structure with a wide angle (Figure S1B), which may be the combination of the effect of the Pro on the peptide's backbone with the hindrance of the side chains of B7-005 residues. On the other hand, when SDS is added to the medium, changes of the B7-005 CD spectrum indicate a conformational change suggesting its interaction with the micelles. In fact, the spectrum no more resembles to that of a type II polyproline helix. We can speculate that the amphipathic environment due to SDS micelles may stabilize different pro-induced conformations, like the type III β-turns that, if recurring, could partially impart a $3_{10}$ helical shape to the peptide [45]. However, further structural studies on B7-005 in the presence of bacterial membranes are desirable to explore its behaviour as a compound that may target, either primarily or secondarily, the bacterial envelope. Membrane targeting indeed appeared to play a prominent role in *S. aureus*, *P. aeruginosa*, *E. cloacae*, and *A baumannii* indicating that, toward these ESKAPE pathogens, B7-005 acts differently than in *E. coli* and *K. pneumoniae*.

*Staphylococcus aureus* and *P. aeruginosa* are susceptible to the peptide at 16 μM. At this concentration, the membrane of both bacteria appeared strongly permeabilized and a low amount of peptide was detected inside bacteria (Fig. 5D, E). This result is consistent with a previous study showing that the PrAMPs Bac7(1–35) killed *P. aeruginosa* clinical isolates shifting its mode of action from intracellular activity to a primarily membrane damage [46]. According to our data, this conclusion can be extended to B7-005 and applies to *S. aureus* as well.

Unexpectedly, a membrane-permeabilization-based mode of action was also observed in the Gram-negative *A. baumannii* and in the Enterobacteriacea *E. cloacae*. This study shows that B7-005 clearly affects *A. baumannii* through a membranolytic mechanism at MIC concentrations as low as 4 μM, which is lower than that required for the killing of *S. aureus* and *P. aeruginosa*. As in these two latter bacteria, the stronger permeabilizing effect on *A. baumannii* corresponded to a reduced amount of peptide inside the bacterial cells. Also *E. cloacae*, despite being closely related to *E. coli* and *K. pneumoniae*, was unexpectedly easily permeabilized by the peptide at MIC (8 μM) and even at sub-MIC (2 μM), strongly supporting a mode of action based on membrane damage. The susceptibility of *E. cloacae* to B7-005 had never been previously tested, but it was reasonable to expect a behaviour similar to that observed on *E. coli* and *K. pneumoniae*.

We then reasoned if the varying susceptibility of different bacterial species to B7-005 and the diversified peptide internalization could be correlated to the presence of a functional SbmA/BacA transporter, which may facilitate the peptide's crossing of the bacterial envelope. Indeed, *E. coli* and *S. typhimurium* possess this permease, allowing PrAMPs to reach the cytoplasm of target cells and to act on ribosomes [47]. Although SbmA was not necessary for B7-005 to target *E. coli* [30], we cannot exclude that its presence could help its activity, especially toward other bacterial species where its mode of action is much less explored than in *E. coli*.

*Staphylococcus aureus* and *P. aeruginosa* do not express SbmA/BacA homologues, which correlates with the limited presence of B7-005 inside their cells and its predominant activity on the membrane. Conversely, *E. cloacae*, closely related to *E. coli* and *K. pneumoniae* as member of the Enterobacteraceae family, encodes a SbmA protein with high identity to that of *E. coli* (Fig. S2). Several key residues in *E. coli* SbmA, identified as essential for transport function [12, 48], are conserved among *E. cloacae*, *E. coli*, and *K.*

*pneumoniae* (Fig. S2). Despite this similarity, our data indicate that the mode of action of B7-005 against *E. cloacae* resembles the lytic mechanism observed in *S. aureus* and *P. aeruginosa* more than the non-lytic mechanism exhibited toward *E coli* and *K pneumoniae*. It is possible that the SbmA homologue in *E. cloacae* is non-functional, has altered specificity, or it is not expressed under the conditions used in this study.

Also, *A. baumanni* possesses a SbmA-homologue protein with 55% of identity with *E. coli* SbmA (see Fig. S2), but the mode of action of B7-005 toward this pathogen is lytic. Previously, the activity of the other PrAMP Bac7(1–35) against clinical isolates of *A. baumannii* was correlated with the grade of peptide internalization [49]; however, there is no indication that data collected for Bac7(1–35) may be extended to B7-005. Moreover, there is no direct evidence that the *A. baumannii* SbmA-like protein is involved in the transport of PrAMPs. In any case, the mere presence of *sbmA* in the genome of bacterial species does not seem to predict sensitivity to, and the mode of action of, B7-005.

In vitro protein synthesis assays, using purified ribosomes extracted from all ESKAPE + E species, demonstrated that B7-005 inhibits translation in all these bacterial species, albeit with varying efficacy (Fig. 6). Moreover, data from toe-printing analysis using *E. coli* ribosomes indicate that B7-005 inhibits protein synthesis by preventing ribosomes from entering the elongation phase (Fig. 7). This mechanism of inhibition is consistent with previous molecular dynamic studies predicting the interaction of B7-005 with the ribosomal exit tunnel [30], and it resembles the inhibition observed with other mammalian and some insect PrAMPs [28].

Although B7-005 has the potential to inhibit protein synthesis in all the ESKAPE + E, if membrane permeabilization occurs at bactericidal concentrations of peptide, the inhibition of translation may serve as a secondary mechanism contributing to bacterial killing. In such cases, B7-005 might passively diffuse through destabilized bacterial membranes, reach the cytosol, and subsequently target the ribosome. It is challenging to determine the relative importance of this secondary mechanism compared to the membranolytic effect in *S. aureus*, *P. aeruginosa*, *A. baumannii*, and *E. cloacae*. Some insights may be gained by comparing the efficacy of B7-005 in inhibiting protein synthesis. *Escherichia coli* and *K. pneumoniae*, which suffered strong inhibition of the protein synthesis in vitro, are also the bacteria most susceptible to B7-005, where killing activity was clearly attributed to a non-lytic mode of action. In the cases of *A. baumannii* and *E. cloacae*, the inhibition of translation is relevant but less pronounced than in *E. coli* and *K. pneumoniae*, happening in the mid-or in the high micromolar range, respectively. This suggests that protein synthesis inhibition may also contribute to, and combine with, membrane permeabilization in the B7-005 bactericidal mechanism. Interestingly, *S. aureus* and *P. aeruginosa*, which appear to be less affected by the inhibition of protein synthesis, were only moderately sensitive to B7-005 as whole bacterial cells, further suggesting that their killing is likely based on membranolytic effects. Notably, *E. faecium*, despite displaying an inhibition of the protein synthesis that is quite similar to what reported for *A. baumannii*, it was only weakly sensitive to B7-005, suggesting that other factors not involving the ribosomes negatively influence the peptide's activity toward this species.

B7-005 displayed high efficacy in inhibiting bacterial translation occurring on the ribosomes of *E. coli* and *K. pneumoniae* (Fig. 6). This paralleled interestingly with the antimicrobial effect of B7-005, since these two *Enterobacteriaceae* were the microorganisms most sensitive to the compound, with MIC of 1 μM or 2 μM, respectively (Table 2). The same strains were also the only ones affected by B7-005 via non-lytic mode of action.

Within this framework, additional insights have been gained by killing kinetics data of B7-005 against different pathogens. Most of 3 $\log_{10}$ drop in bacterial viability (≥) observed within 1 h for *E. cloacae*, *P. aeruginosa*, and *A. baumannii* exposed to 4× MIC aligns with the potent impact that a primarily membrane-active compound can exert on Gram-negative bacteria (Fig. 1C, E, F). Similarly, *S. aureus*, which is also affected by B7-005 via membranolysis, exhibited a rapid decline in viable cells within the same timeframe at 4× MIC (Fig. 1E).

On the other hand, *E. coli*, which is targeted by B7-005 primarily through a non-lytic mechanism, also experienced a rapid and substantial reduction in viability (~ 2.5 $\log_{10}$ within 1 h at 4× MIC) (Fig. 1A). This was expected, as B7-005 was optimized for antimicrobial potency using *E. coli* as a reference strain. It is therefore unsurprising that the peptide exerts a powerful and rapid antibacterial effect against this species, efficiently inhibiting protein synthesis while also maybe lightly perturbing (although not damaging) its bacterial membrane.

Interestingly, *K. pneumoniae* does not fit neatly into either of these models. After 1 h of exposure to B7-005 at 4× MIC, bacterial viability remained unchanged, and even after 4 h, the reduction was below 2 log10 (Fig. 1B). However, despite this slow onset, B7-005 exhibited both inhibitory and bactericidal activity against *K. pneumoniae* at relatively low concentrations after long incubations (MIC = 2 μM, MBC = 4 μM), suggesting a delayed killing effect. Since *K. pneumoniae* is affected by B7-005 through a non-lytic mechanism (Fig. 5B) and its ribosomes are highly susceptible to inhibition (Fig. 6), we hypothesize that its slow killing kinetics may result from a low rate of peptide uptake. Flow cytometry data support this idea, revealing that the amount of B7-005 internalized by *K. pneumoniae* was approximately half of what is observed in *E. coli* at the same timepoints (Fig. 5A, B).

We cannot be strictly dichotomous in defining the mode of action of B7-005, therefore relying exclusively either on

protein synthesis inhibition or membrane disruption. Rather, these mechanisms may variate according to the target pathogens and also be interconnected. Once internalized, B7-005 could effectively inhibit the ribosomes of pathogens beyond *E. coli* and *K. pneumoni*ae (Fig. 6), suggesting the possibility of a combined mode of action.

From a phylogenetic perspective, the distance from *E. coli* therefore is not predictive for the inhibiting activity of B7-005 on the protein synthesis. B7-005 still displayed a relevant inhibiting potency on *A. baumannii* ribosomes (Fig. 6), and this may contribute in making this microorganism one of the most sensitive toward B7-005 among the ESKAPE + E (Table 2). One could speculate that *A. baumannii* represents an example of mixed activity of B7-005. The peptide could combine a first membranolytic effect with a secondary inhibition of the ribosomal activity, after seeping into the cytosol through the damaged membrane. A similar reasoning could be applied to *E. cloacae*. This specie is phylogenetically closer to *E. coli* and *K. pneumoniae* than *A. baumanni*, but nevertheless, it is less affected by B7-005 than the aforementioned pathogens considering both the MIC (Table 2) and the inhibition of the protein synthesis (Figs. 6 and 7). Interestingly, *S. aureus* and *P. aeruginosa*, that were only moderately sensitive to B7-005 as living cells (Table 2), were also poorly affected by the peptide on their protein synthesis (Fig. 6). Further studies on the molecular details of the ribosome by B7-005 on the ESKAPE + E will be stimulating for the design of new protein synthesis inhibitors.

In conclusion, this study highlights how the mode of action of this peptide differs from that of other PrAMPs. The potency and molecular mechanism of B7-005 against the ESKAPE + E pathogens changes more or less distinctly depending on the type of bacterial species. The mode of action ranges from a purely intracellular inhibitor to a completely permeabilizing peptide, passing through intermediate conditions, where killing likely occurs via both mechanisms. This property could be very important for countering the emergence of resistance phenomena. In this regard, B7-005 has already demonstrated, albeit only in *E. coli*, that it is a peptide against which it is difficult to develop resistance [22]. Nonetheless, a deeper understanding of the molecular interactions of this peptide with its targets will allow for modifications to tailor it to the characteristics of each of these pathogens, ultimately leading to the development of more effective new antibiotics.

**Supplementary Information** The online version contains supplementary material available at https://doi.org/10.1007/s12602-025-10568-5.

**Acknowledgements** We thank Prof. Marco Gerdol for help with the sequence alignment (Fig S2), Dr. Andrea Caporale and Anna Perrone for assistance with circular dichroism analysis and Prof Alessandro Tossi for critically reading the manuscript.

**Author Contribution** ADS, MS MMa conceptualized the project. ADS, SC, MMo, SB, MB, SP, TDP, AF, MMa performed the experiments, analysed the data and prepared the Figures. PM, DNW, RS, MS, MMa provided funding and resources. MMa, MS, ADS wrote the original draft. PM, DNW, AF, MS, MMa supervised the project. All the authors edited the final version of the article.

**Funding** Open access funding provided by Università degli Studi di Trieste within the CRUI-CARE Agreement. This study was supported by the following grants:

Programma Regionale (PR) FSE + 2021/2027, grant of Regione Autonoma Friuli Venezia Giulia—PPO 2023—Specific Program 22/23—decreto n.17895/GRFVG dd.19.04.2023. "Integrated approach to control and prevent of the antibiotic-resistance infections" to Marco Scocchi.

Progetti di Ricerca di Rilevante Interesse Nazionale—PRIN2022 Project 2022EKWRHB, grant of the Italian Ministry of University and Research to Mario Mardirossian.

Progetti di Ricerca di Rilevante Interesse Nazionale—PRIN2022 Project—2022XFFTH5, grant of the Italian Ministry of University and Research to Marco Scocchi.

Deutsche Forschungsgemeinschaft (DFG) grant, WI3285/12–1 to Daniel N. Wilson.

**Data Availability** No datasets were generated or analysed during the current study.

## Declarations

**Competing Interests** The authors declare no competing interests.



## References

1. De Oliveira DMP, Forde BM, Kidd TJ, Harris PNA, Schembri MA, Beatson SA, Paterson DL, Walker MJ (2020) Antimicrobial resistance in ESKAPE pathogens. Clin Microbiol Rev 33:e00181-e219. https://doi.org/10.1128/CMR.00181-19
2. Mulani MS, Kamble EE, Kumkar SN, Tawre MS, Pardesi KR (2019) Emerging strategies to combat ESKAPE pathogens in the era of antimicrobial resistance: a review. Front Microbiol 10:539. https://doi.org/10.3389/fmicb.2019.00539
3. Santajit S, Indrawattana N (2016) Mechanisms of antimicrobial resistance in ESKAPE pathogens. Biomed Res Int 2016:e2475067. https://doi.org/10.1155/2016/2475067
4. Mahlapuu M, Björn C, Ekblom J (2020) Antimicrobial peptides as therapeutic agents: opportunities and challenges. Crit Rev Biotechnol 40:978–992. https://doi.org/10.1080/07388551.2020.1796576
5. Magana M, Pushpanathan M, Santos AL, Leanse L, Fernandez M, Ioannidis A, Giulianotti MA, Apidianakis Y, Bradfute S, Ferguson

AL et al (2020) The value of antimicrobial peptides in the age of resistance. Lancet Infect Dis 20:e216–e230. https://doi.org/10.1016/S1473-3099(20)30327-3
6. Lazzaro BP, Zasloff M, Rolff J (2020) Antimicrobial peptides: application informed by evolution. Science 368:eaau5480. https://doi.org/10.1126/science.aau5480
7. Kumar P, Kizhakkedathu JN, Straus SK (2018) Antimicrobial peptides: diversity, mechanism of action and strategies to improve the activity and biocompatibility in vivo. Biomolecules 8:4. https://doi.org/10.3390/biom8010004
8. Sani M-A, Separovic F (2016) How membrane-active peptides get into lipid membranes. Acc Chem Res 49:1130–1138. https://doi.org/10.1021/acs.accounts.6b00074
9. Scocchi M, Mardirossian M, Runti G, Benincasa M (2016) Non-membrane permeabilizing modes of action of antimicrobial peptides on bacteria. Curr Top Med Chem 16:76–88
10. Graf M, Mardirossian M, Nguyen F, Seefeldt AC, Guichard G, Scocchi M, Innis CA, Wilson DN (2017) Proline-rich antimicrobial peptides targeting protein synthesis. Nat Prod Rep 34:702–711. https://doi.org/10.1039/c7np00020k
11. Mardirossian M, Grzela R, Giglione C, Meinnel T, Gennaro R, Mergaert P, Scocchi M (2014) The host antimicrobial peptide Bac71-35 binds to bacterial ribosomal proteins and inhibits protein synthesis. Chem Biol 21:1639–1647. https://doi.org/10.1016/j.chembiol.2014.10.009
12. Mattiuzzo M, Bandiera A, Gennaro R, Benincasa M, Pacor S, Antcheva N, Scocchi M (2007) Role of the *Escherichia coli* SbmA in the antimicrobial activity of proline-rich peptides. Mol Microbiol 66:151–163. https://doi.org/10.1111/j.1365-2958.2007.05903.x
13. Krizsan A, Knappe D, Hoffmann R (2015) Influence of the yjiL-mdtM gene cluster on the antibacterial activity of proline-rich antimicrobial peptides overcoming *Escherichia coli* resistance induced by the missing SbmA transporter system. Antimicrob Agents Chemother 59:5992–5998. https://doi.org/10.1128/AAC.01307-15
14. Krizsan A, Volke D, Weinert S, Sträter N, Knappe D, Hoffmann R (2014) Insect-derived proline-rich antimicrobial peptides kill bacteria by inhibiting bacterial protein Translation at the 70 S Ribosome. Angew Chem Int Ed 53:12236–12239. https://doi.org/10.1002/anie.201407145
15. Gagnon MG, Roy RN, Lomakin IB, Florin T, Mankin AS, Steitz TA (2016) Structures of proline-rich peptides bound to the ribosome reveal a common mechanism of protein synthesis inhibition. Nucleic Acids Res 44:2439–2450. https://doi.org/10.1093/nar/gkw018
16. Mardirossian M, Barrière Q, Timchenko T, Müller C, Pacor S, Mergaert P, Scocchi M, Wilson DN (2018) Fragments of the nonlytic proline-rich antimicrobial peptide Bac5 kill Escherichia coli cells by inhibiting protein synthesis. Antimicrob Agents Chemother 62. https://doi.org/10.1128/AAC.00534-18
17. Roy RN, Lomakin IB, Gagnon MG, Steitz TA (2015) The mechanism of inhibition of protein synthesis by the proline-rich peptide oncocin. Nat Struct Mol Biol 22:466–469. https://doi.org/10.1038/nsmb.3031
18. Scocchi M, Tossi A, Gennaro R (2011) Proline-rich antimicrobial peptides: converging to a non-lytic mechanism of action. Cell Mol Life Sci 68:2317–2330. https://doi.org/10.1007/s00018-011-0721-7
19. Benincasa M, Scocchi M, Podda E, Skerlavaj B, Dolzani L, Gennaro R (2004) Antimicrobial activity of Bac7 fragments against drug-resistant clinical isolates. Peptides 25:2055–2061. https://doi.org/10.1016/j.peptides.2004.08.004
20. Mardirossian M, Sola R, Beckert B, Valencic E, Collis DWP, Borišek J, Armas F, Di Stasi A, Buchmann J, Syroegin EA et al (2020) Peptide inhibitors of bacterial protein synthesis with broad spectrum and SbmA-independent bactericidal activity against clinical pathogens. J Med Chem 63:9590–9602. https://doi.org/10.1021/acs.jmedchem.0c00665
21. Mardirossian M, Gruppuso M, Guagnini B, Mihalić F, Turco G, Porrelli D (2023) Advantages of agarose on alginate for the preparation of polysaccharide/hydroxyapatite porous bone scaffolds compatible with a proline-rich antimicrobial peptide. Biomed Mater 18:065018. https://doi.org/10.1088/1748-605X/ad02d3
22. Di Stasi A, Bozzer S, Pacor S, De Pascale L, Morici M, Favero L, Spazzapan M, Pegoraro S, Bulla R, Wilson DN et al (2024) The proline-rich antimicrobial peptide B7–005: low bacterial resistance, safe for human cells and effective in zebrafish embryo bacteraemia model. Open Biol 14:240286. https://doi.org/10.1098/rsob.240286
23. Kuipers BJH, Gruppen H (2007) Prediction of molar extinction coefficients of proteins and peptides using UV absorption of the constituent amino acids at 214 nm to enable quantitative reverse phase high-performance liquid chromatography−mass spectrometry analysis. J Agric Food Chem 55:5445–5451. https://doi.org/10.1021/jf070337l
24. Guida F, Benincasa M, Zahariev S, Scocchi M, Berti F, Gennaro R, Tossi A (2015) Effect of size and N-terminal residue characteristics on bacterial cell penetration and antibacterial activity of the proline-rich peptide Bac7. J Med Chem 58:1195–1204. https://doi.org/10.1021/jm501367p
25. Sola R, Mardirossian M, Beckert B, Sanghez De Luna L, Prickett D, Tossi A, Wilson DN, Scocchi M (2020) Characterization of cetacean proline-rich antimicrobial peptides displaying activity against ESKAPE pathogens. IJMS 21:7367. https://doi.org/10.3390/ijms21197367
26. Mardirossian M, Sola R, Degasperi M, Scocchi M (2019) Search for shorter portions of the proline-rich antimicrobial peptide fragment Bac 5(1–25) that retain antimicrobial activity by blocking protein synthesis. ChemMedChem 14:343–348. https://doi.org/10.1002/cmdc.201800734
27. Abramson J, Adler J, Dunger J, Evans R, Green T, Pritzel A, Ronneberger O, Willmore L, Ballard AJ, Bambrick J et al (2024) Accurate structure prediction of biomolecular interactions with AlphaFold 3. Nature 630:493–500. https://doi.org/10.1038/s41586-024-07487-w
28. Koller TO, Morici M, Berger M, Safdari HA, Lele DS, Beckert B, Kaur KJ, Wilson DN (2023) Structural basis for translation inhibition by the glycosylated drosocin peptide. Nat Chem Biol 19:1072–1081. https://doi.org/10.1038/s41589-023-01293-7
29. Seefeldt AC, Nguyen F, Antunes S, Pérébaskine N, Graf M, Arenz S, Inampudi KK, Douat C, Guichard G, Wilson DN et al (2015) The proline-rich antimicrobial peptide Onc112 inhibits translation by blocking and destabilizing the initiation complex. Nat Struct Mol Biol 22:470–475. https://doi.org/10.1038/nsmb.3034
30. Mardirossian M, Sola R, Beckert B, Valencic E, Collis DWP, Borišek J, Armas F, Di Stasi A, Buchmann J, Syroegin EA et al (2020) Peptide inhibitors of bacterial protein synthesis with broad spectrum and SbmA-independent bactericidal activity against clinical pathogens. J Med Chem 63:9590–9602. https://doi.org/10.1021/acs.jmedchem.0c00665
31. Woody RW (2009) Circular dichroism spectrum of peptides in the poly(Pro)II conformation. J Am Chem Soc 131:8234–8245. https://doi.org/10.1021/ja901218m
32. Chiba S, Kanamori T, Ueda T, Akiyama Y, Pogliano K, Ito K (2011) Recruitment of a species-specific translational arrest module to monitor different cellular processes. Proc Natl Acad Sci USA 108:6073–6078. https://doi.org/10.1073/pnas.1018343108
33. Shimokawa-Chiba N, Müller C, Fujiwara K, Beckert B, Ito K, Wilson DN, Chiba S (2019) Release factor-dependent ribosome rescue by BrfA in the Gram-positive bacterium Bacillus subtilis. Nat Commun 10:5397. https://doi.org/10.1038/s41467-019-13408-7

34. Goudarzi M, Khoshbayan A, Taheri F (2021) Retapamulin: current status and future perspectives. Arch Clin Infect Dis 16:e114970. https://doi.org/10.5812/archcid.114970
35. Seefeldt AC, Graf M, Pérébaskine N, Nguyen F, Arenz S, Mardirossian M, Scocchi M, Wilson DN, Innis CA (2016) Structure of the mammalian antimicrobial peptide Bac 7(1–16) bound within the exit tunnel of a bacterial ribosome. Nucleic Acids Res 44:2429–2438. https://doi.org/10.1093/nar/gkv1545
36. Mardirossian M, Pérébaskine N, Benincasa M, Gambato S, Hofmann S, Huter P, Müller C, Hilpert K, Innis CA, Tossi A et al (2018) The dolphin proline-rich antimicrobial peptide Tur1A inhibits protein synthesis by targeting the bacterial ribosome. Cell Chem Biol 25:530-539.e7. https://doi.org/10.1016/j.chembiol.2018.02.004
37. Mardirossian M, Barrière Q, Timchenko T, Müller C, Pacor S, Mergaert P, Scocchi M, Wilson DN (2018) Fragments of the nonlytic proline-rich antimicrobial peptide Bac5 kill *Escherichia coli* cells by inhibiting protein synthesis. Antimicrob Agents Chemother 62. https://doi.org/10.1128/AAC.00534-18
38. Wu H, Huang J (2018) Optimization of protein and peptide drugs based on the mechanisms of kidney clearance. PPL 25:514–521. https://doi.org/10.2174/0929866525666180530122835
39. Schmidt R, Ostorházi E, Wende E, Knappe D, Hoffmann R (2016) Pharmacokinetics and *in vivo* efficacy of optimized oncocin derivatives. J Antimicrob Chemother 71:1003–1011. https://doi.org/10.1093/jac/dkv454
40. Mardirossian M, Pompilio A, Crocetta V, De Nicola S, Guida F, Degasperi M, Gennaro R, Di Bonaventura G, Scocchi M (2016) *In vitro* and *in vivo* evaluation of BMAP-derived peptides for the treatment of cystic fibrosis-related pulmonary infections. Amino Acids 48:2253–2260. https://doi.org/10.1007/s00726-016-2266-4
41. Benincasa M, Lagatolla C, Dolzani L, Milan A, Pacor S, Liut G, Tossi A, Cescutti P, Rizzo R (2016) Biofilms from *Klebsiella pneumoniae*: matrix polysaccharide structure and interactions with antimicrobial peptides. Microorganisms 4:26. https://doi.org/10.3390/microorganisms4030026
42. Guerra MES, Destro G, Vieira B, Lima AS, Ferraz LFC, Hakansson AP, Darrieux M, Converso TR (2022) *Klebsiella pneumoniae* biofilms and their role in disease pathogenesis. Front Cell Infect Microbiol 12:877995. https://doi.org/10.3389/fcimb.2022.877995
43. De Souza CM, Da Silva ÁP, Júnior NGO, Martínez OF, Franco OL (2022) Peptides as a therapeutic strategy against Klebsiella pneumoniae. Trends Pharmacol Sci 43:335–348. https://doi.org/10.1016/j.tips.2021.12.006
44. De Los Santos L, Beckman RL, DeBarro C, Keener JE, Torres MDT, Fuente-Nunez CDL, Brodbelt JS, Fleeman RM (2024) Polyproline peptide targets *Klebsiella pneumoniae* polysaccharides to collapse biofilms. Cell Rep Phys Sci 5:101869. https://doi.org/10.1016/j.xcrp.2024.101869
45. Pal L, Basu G, Chakrabarti P (2002) Variants of $3_{10}$-helices in proteins. Proteins 48:571–579. https://doi.org/10.1002/prot.10184
46. Runti G, Benincasa M, Giuffrida G, Devescovi G, Venturi V, Gennaro R, Scocchi M (2017) The mechanism of killing by the proline-rich peptide Bac7(1–35) against clinical strains of *Pseudomonas aeruginosa* differs from that against other Gram-negative bacteria. Antimicrob Agents Chemother 61. https://doi.org/10.1128/AAC.01660-16
47. Graf M, Mardirossian M, Nguyen F, Seefeldt AC, Guichard G, Scocchi M, Innis CA, Wilson DN (2017) Proline-rich antimicrobial peptides targeting protein synthesis. Nat Prod Rep 34:702–711. https://doi.org/10.1039/C7NP00020K
48. Ghilarov D, Inaba-Inoue S, Stepien P, Qu F, Michalczyk E, Pakosz Z, Nomura N, Ogasawara S, Walker GC, Rebuffat S et al (2021) Molecular mechanism of SbmA, a promiscuous transporter exploited by antimicrobial peptides. Sci Adv 7:eabj5363. https://doi.org/10.1126/sciadv.abj5363e
49. Dolzani L, Milan A, Scocchi M, Lagatolla C, Bressan R, Benincasa M (2019) Sub-MIC effects of a proline-rich antibacterial peptide on clinical isolates of *Acinetobacter baumannii*. J Med Microbiol 68:1253–1265. https://doi.org/10.1099/jmm.0.001028